VARIATION OF THE ENHANCED BIOLOGICALLY DAMAGING SOLAR UV DUE TO CLOUDS

Parisi, A.V[a,#]., Downs, N[a]

[a]Centre for Astronomy, Solar Radiation and Climate, University of Southern Queensland, Toowoomba, 4350, Australia. Ph: 61 7 4631 2226. FAX: 61 7 4631 2721. Email: parisi@usq.edu.au

[#]To whom correspondence should be addressed.

Parisi, Alfio and Downs, N. (2004) *Variation of the enhanced biologically damaging solar UV due to clouds.* Photochemical and Photobiological Sciences, 3. pp. 643-647.
Authors' final manuscript version.

Abstract

The variation of the biologically damaging solar UV (UVBE) enhanced by clouds above that of clear sky UVBE has been investigated. This was undertaken for summer through to winter for SZA of 5 to 60^{o} employing an integrated automatic cloud and spectral UV measurement system that recorded the solar UV spectra and the sky images at five minute intervals. The UVBE calculated with action spectra with higher relative effectiveness in the UVA produced the lower percentage of cloud enhanced cases. The DNA UVBE provided the highest percentage of cloud enhanced cases compared to the total number of UV scans with 2.2% cloud enhanced cases. As a comparison, the plant and fish melanoma UVBE provided the lowest percentage of cloud enhanced cases with 0.6% to 0.8% cloud enhanced cases. For the cases of cloud enhanced UVBE, the average ratio of the measured UVBE to calculated cloud free UVBE for the photokeratitis, cataracts, plant, generalized plant damage and fish melanoma action spectra was 1.21 to 1.25. In comparison, the highest value of 1.4 was for the DNA action spectrum.

Introduction

Previous research has reported the increase or enhancement due to clouds of the solar UV radiation above that of a cloud free day. A review of research in this field has been provided in Parisi et al.[1] Previous research has reported an increase of UV above that of a cloud free day, referred to in this paper as cloud enhanced UV (for example, 2-7). Enhancements in the six minute irradiance measurements of the UVB (280-320 nm) waveband at a sub-tropical site over a twelve month period had an occurrence of 3% with maximum enhancements by a factor of 1.4 compared to the respective clear sky irradiances.[5] At the same location, the cloud enhanced UVA (320-400 nm) irradiances were investigated over autumn and winter[3] and for three days found to add to 134.6 kJ m^{-2} above that of clear sky days with the maximum enhancements by a factor of 1.08 compared to the respective clear sky irradiances. UVB enhancements due to cloud of 115% compared to a cloud free sky were reported at a northern hemisphere site (47.4^{o}N) for solar elevations of less than 30^{o} and cloud cover of 25%.[8]

Cloud enhanced erythemal UV has been measured for cloud cover between two and eight oktas.[6] UV enhancement by cloud has been reported to occur when the solar disc is obscured, but may still be visible through cirrus cloud or haze.[5] Additionally, cloud enhanced erythemal UV, along with cloud enhanced global solar radiation (0.3-3 μm) has been measured when the solar disc is clear of clouds and the diffuse component of the solar UV is increased when there is cloud near the sun such as broken or thin cloud.[5,7] In these cases, as the fraction cloud cover increases, there is a tendency for the cloud enhancements of the global radiation to be higher.[5,9]

The absorption of UV by important biological macromolecules is wavelength specific. In order to calculate the biologically damaging UV (UVBE) for a specific process, it is necessary to weight the incident spectral irradiance with a dimensionless function called the action spectrum, A(λ). The relative shapes of the different action spectra are dependent on the biologically damaging process that they are describing. Sabburg et al.[4] has reported marginally higher UV enhancements and frequency in the UVB compared to the UVA. This research also found the UV enhancements to be wavelength independent for wavelengths longer than 306 nm and increasingly wavelength dependent for shorter wavelengths. This wavelength dependency at the shorter wavelengths suggests that the properties of the cloud enhanced UVBE will be influenced by the action spectrum under consideration.

This previous research has considered the effect of enhancements due to cloud on the broadband UVA and UVB, erythemal UV and unweighted spectral UV. The research reported in this study extends this previous research to consider the effects of the enhancements due to cloud on the UVBE that has been weighted with six different action spectra for biological effects on human skin and eyes and plants.

Materials and Methods

Integrated Cloud and Spectral UV Equipment

A synchronized integrated automatic cloud and spectral UV measurement system as described elsewhere[10] was employed. Briefly, the system consisted of a UV spectroradiometer (model DTM300, Bentham Instruments, Reading, UK) and a Total Sky Imager (TSI) (model TSI-440, Yankee Environmental Systems, MA, USA) concurrently

collecting an image of the sky for analysis of the percentage cloud cover. The spectroradiometer automatically collected the UV spectrum from 280 to 400 nm in 0.5 nm increments every five minutes and the TSI automatically collected and analysed a sky image every five minutes for amount of cloud cover within a 160^{o} field of view. Each spectral UV scan takes approximately 2 minutes plus approximately another minute for the initialisation of the scan. Each TSI image is scheduled to be taken at the start of the spectral UV scan. The equipment is on the unobstructed roof of a building at the University of Southern Queensland, Toowoomba, (27.5 ^{o}S, 693 m above sea level) Australia. The control and data acquisition software of both the spectroradiometer and TSI are on the same computer to provide a synchronized integrated system.

The data set in this paper spans the period from 1 January 2003 to 30 June 2003. The instrument was irradiance calibrated on 17 March 2003 against a 150 W quartz tungsten halogen (QTH) lamp calibrated to the National Physical Laboratory, UK standard and wavelength calibrated against the UV spectral lines of a mercury lamp. On a fortnightly to monthly basis, the stability and wavelength calibration of the instrument was checked against 150 W QTH lamps and the mercury lamp UV spectral lines respectively. The irradiance uncertainty of the Bentham spectroradiometer was of the order of ±6% based on the temporal stability, cosine error and dark count variability. The temporal variability was calculated as the averaged percentage change in the measured output of the 150 W QTH lamps. The cosine error was taken as the largest error between the manufacturer supplied response and the cosine function for angles between 0 and 70^{o} to the normal. The dark count variability was the maximum variability of the dark count about the mean dark count over the temperature range of 5 to 24 ^{o}C. The uncertainty in the absolute irradiance calibration of the spectroradiometer was an additional ±3%. This research deals with the comparison of the data from spectra collected by this instrument, instead of absolute irradiances and consequently the uncertainty figure of ±6% will be employed for the UVBE irradiances in the determination of the cloud enhanced cases.

The TSI consists of a charged couple device (CCD) camera mounted over a hemispheric mirror. An example of an unprocessed and a processed image are shown in Figure 1. The camera is mounted over the mirror with a thin pipe that is attached to the base of the TSI and is seen as a thin line from the bottom to the centre of the image. The thick black band is a shadow band used to obscure the sun. It is taped to the hemispheric mirror and the mirror rotates to track the sun. Both the shadow band and the camera support are masked in the image processing and calculation of the fractional cloud cover and correspond to approximately 9% of the image. In the processed image, the clouds are represented as white and the cloud free areas are dark. In this example the fractional cloud cover has been calculated as 72%. The automated TSI removes the problem of cost and subjectivity associated with manual observations of the cloud cover.

Biologically Damaging UV

For a particular action spectrum, A(λ), the biologically damaging UV irradiance, UVBE, is calculated employing:

$$UVBE = \int_{UV} S(\lambda)A(\lambda)d\lambda \qquad \text{W m}^{-2} \qquad (1)$$

where $S(\lambda)$ is the measured spectral irradiance and $d\lambda$ is the wavelength increment of the spectral data, 0.5 nm in this case. Practically, the integration is replaced by the summation over the UV waveband and $d\lambda$ by $\Delta\lambda$. The summation is either over the range 290 to 400 nm or 290 nm to the longest wavelength that the respective action spectrum extends to.

In this research, the UVBE for human skin and eyes and for plants has been considered. This research employs the action spectra for generalized plant damage,[11] plant damage,[12] DNA damage,[13] fish melanoma,[14] photokeratitis[15] and cataracts[16] (Figure 2). No action spectrum exists for cataract formation in humans and the action spectrum for in-vitro cataract formation in a cultured porcine lens has been employed as the pig's lens is similar in shape and size to the human lens, allowing inferences to be made with the lens of humans.[16] Similarly, there is no $A(\lambda)$ for human melanoma, however the fish melanoma $A(\lambda)$ shows that the UVA wavelengths are implicated in the induction of melanoma in this species and may provide an indication of the wavelengths effective in producing human melanoma.[17] The generalized plant damage action spectrum[11] which is zero for wavelengths longer than 313 nm is the average of nine different plant UVB responses and has been widely employed in the determination of plant responses to increased UVB. The action spectrum by Flint and Caldwell,[12] has been proposed for plant growth responses in higher plants with a response extending to 366 nm. In the following, this action spectrum will be referred to as the plant action spectrum.

A function that is available in the literature for each of the action spectra for generalized plant damage,[18] plant damage[12] and DNA damage[19] has been employed to calculate these action spectra. For the other action spectra, linear interpolation between the data points available in the literature has been employed. These six action spectra have been selected as they provide a range of biologically damaging effects for human skin and eyes and plants and additionally, the range of the relative effectiveness covers both the UVB and UVA wavebands.

Cloud Enhanced UVBE

The UVBE was calculated for each of the measured spectra and the cases of cloud enhanced UVBE were determined by first establishing the cloud free envelope for the UVBE for each action spectrum. For each five minute UVBE irradiance for the respective action spectrum, the data from the TSI was employed to determine if it was collected during a cloud free period. A spectral UV scan was classified as cloud free if the processed sky image analysed by the TSI software recorded less than 2% opaque cloud and less than 2% thin cloud provided the solar disc was not obstructed.

The statistical package SPSS version 11.5 was employed for data analysis and fitting of a cubic regression curve to the cloud free data for each action spectrum. A cubic function was employed as it provided a reasonable fit as determined by the R^2 value without having to employ a complex function. As the curve was fitted to the measured data, it takes into account the variation in the sun-earth distance. The fitted curve was a function of SZA and allowed calculation of the cloud free envelope of the UVBE for any SZA at which a UV spectrum was collected. For each of the UVBE irradiances that were classified as cloud free, the difference between the measured UVBE and the UVBE calculated with the fitted curve employing the appropriate SZA was determined. For each dataset, the 95^{th} percentile (p0.95) of these differences was determined. This was to provide an estimate of the variation of the cloud free irradiances due to errors in the spectral data and atmospheric variations due to changes in aerosols and ozone. For any measured data point ($UVBE_{Meas}$), the following rule was employed to determine if it was a case of cloud enhancement:

$$\left[UVBE_{Meas} - 0.06 \times UVBE_{Meas}\right] > \left[UVBE_{Clear} + p0.95\right] \quad (2)$$

where $UVBE_{Clear}$ is the UVBE calculated with the fitted curve representing the cloud free envelope for the SZA corresponding to that for each $UVBE_{Meas}$ data point. The multiplier of 0.06 is used to calculate the lowest value of $UVBE_{Meas}$ as a result of the measurement uncertainty associated with the measured UVBE. Similarly, the addition of p0.95 to $UVBE_{Clear}$ is employed to use the upper uncertainty limit of the cloud free envelope.

Following determination of the cases of cloud enhanced UVBE, the ratio of the measured UVBE to calculated cloud free UVBE of these cases for each action spectrum was calculated as follows:

$$R_{Enh} = \frac{UVBE_{Meas}}{UVBE_{Clear}} \quad (3)$$

Results

Over the six month period, a total of approximately 12,500 UV spectra were recorded. Of these approximately 15.6% were classified as recorded during a cloud free period that was defined using the previously described criteria. The UVBE for plant damage[12] are shown in Figure 3 for both all sky conditions (light shaded symbols) and for the cases classified as cloud free (dark shaded symbols). The spectra classified as cloud free produce a band of UVBE irradiances that varied as a function of the SZA. The width of this band is due to measurement errors and variations in the atmospheric properties due to aerosols and ozone. In this case, the value of p0.95 is 84.3. The cases of cloud enhanced UVBE can be seen above the cloud free irradiances. Some of these cases above the cloud free irradiances are due to genuine cases of cloud enhanced UV and some are due to the measurement uncertainty of ±6%. Similarly, the same situation was applied for the other action spectra.

For the cloud enhanced cases, the ratio of the measured to corresponding clear sky irradiances are shown in Figure 4 to Figure 6. The lower limit of the R_{Enh} ratios tends to higher values as the SZA increases. This is due to the classification rule (Equation 2) where the percentage of p0.95 compared to $UVBE_{Clear}$ increases as the SZA increases. Irrespective of this the values of R_{Enh} increase for increasing SZA. The number of cloud enhanced cases was influenced by the action spectrum under consideration. The DNA UVBE provided the highest percentage of cloud enhanced cases compared to the total number of UV scans with 2.2% of these scans representing cloud enhanced cases. As a comparison, the plant and fish melanoma UVBE provided the lowest percentage of cloud enhanced cases with 0.6% to 0.8% representing cloud enhanced cases. For the DNA UVBE, the number of consecutive spectra that the cloud enhanced effect was found to last was an average of 2.4 spectra with a maximum of 17 spectra where the time period for one spectrum is five minutes. Similarly, for the plant UVBE, the average was 1.4 spectra and the maximum was 10 spectra. Comparing the percentage of cloud enhanced cases for the DNA UVBE to the previously reported percentage of cases for the UVB waveband[5] shows that there is reasonable similarity when considering that measurements were taken in different years when the cloud conditions were different.

The R_{Enh} ratios have been averaged for each of the action spectra and provided in Figure 7 with the error bars representing the standard error in the mean. For the photokeratitis, cataracts, plant, generalized plant damage and fish melanoma action spectra, the average is similar with the range of 1.21 to 1.25. In comparison, the highest value of 1.4 is for the DNA action spectrum.

For the cloud enhanced UV cases, the average of the UVBE irradiances were calculated for each action spectrum. These averages are dependent on the SZA, however, these are provided along with the standard deviations in order to provide information on the magnitude of the range. The values are 6.3 (3) W m^{-2}, 15,654 (3,788) W m^{-2}, 1260 (285) W m^{-2}, 115 (36) W m^{-2}, 312 (116) W m^{-2} and 199 (72) W m^{-2} for the DNA, fish melanoma, plant, generalized plant damage, cataracts and photokeratitis action spectra respectively, where the values in parentheses are the standard deviations.

Discussion

The research in this paper has investigated the variation with clouds of the biologically damaging solar UV for humans and plants. This is the first extensive investigation of the cloud enhanced UVBE for action spectra other than the erythemal action spectrum. This was undertaken for summer through to winter for SZA of 5^o to 60^o employing an integrated automatic cloud and spectral UV measurement system that recorded the solar UV spectra and the sky images at five minute intervals. The period from summer to winter was employed in order to cover the range of SZA encountered at the site of the research between approximately 9 am and noon. This was necessary in order to incorporate the different relative changes in the UVBE exposures for the different action spectra as a result of the changing SZA.[20]

The percentage of cloud enhanced UVBE cases compared to the total number of scans was influenced by the action spectrum employed to calculate the UVBE. The UVBE calculated with action spectra with higher relative effectiveness in the UVA produced the lower percentage of cloud enhanced cases. This is consistent with the finding of Sabburg et al.[4] who reported that the spectral influence of cloud enhanced UV is likely to be higher in the UVB waveband for wavelengths shorter than 306 nm. Additionally, the average and maximum number of consecutive spectra for which the cloud enhanced effect lasts is higher for the action spectrum with the higher relative effectiveness in the UVB. Consequently, the relative UVA to UVB effectiveness of the action spectrum for the biologically damaging process influences the cloud enhanced UV.

The enhanced UVBE is important in the consideration of the biologically damaging UV for humans and plants. This would be further highlighted if the cloud enhanced UVBE irradiances are considered relative to the reduced irradiances that would occur when the redistribution of the same amount of cloud produces a significant reduction in the UVBE. The cloud enhanced DNA UVBE lasted an average of 11.3 minutes with the longest one lasting 85 minutes. Consequently, the cases of cloud enhanced UVBE are significant for processes such as photosynthesis on plants. Similarly, UV radiation is at least one contributing risk factor in the formation of cataracts and cases of cloud enhanced UV may contribute to the threshold UVB exposure for photokeratitis. For humans the risk of squamous cell carcinoma is related to the cumulative exposure to UV radiation. For basal cell carcinoma, evidence suggests that the risk is related to intermittent exposures.[21] The cases of cloud enhanced UV that individuals are exposed to contribute to these risks.

***Acknowledgements*:**
The authors acknowledge Dr Jeff Sabburg and the technical staff in Physics and the Sciences workshop, USQ for their assistance in this project, along with the funding provided by the Australian Research Council for the spectroradiometer and the University of Southern Queensland for the TSI.

References

1. A.V. Parisi, J. Sabburg and M.G. Kimlin, Scattered and Filtered Solar UV Measurements, Kluwer Academic Publishers, Dordrecht, 2004, pp.109-129.
2. J.G. Estupinan, S. Raman, G.H. Crescenti, J.J. Streicher and W.F. Barnard, Effects of cloud and haze on UV-B radiation, *J. Geophys. Res.*, 1996, **104**, 16,807-16,816.
3. J. Sabburg, A.V. Parisi and J. Wong, Effect of cloud on UVA and exposure to humans, *Photochem. Photobiol.*, 2001, **74**, 412-416.
4. J. Sabburg, A.V. Parisi and M.G. Kimlin, Enhanced spectral UV irradiance: a one year preliminary study, *Atmos. Res.*, 2003, **66**, 261-272.
5. J. Sabburg and J. Wong, The effect of clouds on enhancing UVB irradiance at the earth's surface: a one year study, *Geophys. Res. Lett.*, 2000, **27**, 3,337-3,340.
6. S. Thiel, K. Steiner and H.K. Seidlitz, Modification of global erythemally effective irradiance by clouds, *Photochem. Photobiol.*, 1997, **65**, pp.969-973.
7. G. Pfister, R.L. McKenzie, J.B. Liley, A. Thomas, M.J. Uddstrom and A. Heidinger, Cloud climatology for New Zealand and implications for radiation fields, *UV Radiation and its Effects: an update (2002) Conference*, Christchurch, New Zealand. 26-28 Mar. 2002.
8. P. Nemeth, Z. Toth and Z. Nagy, Effect of weather conditions on UV-B radiation reaching the earth's surface, *J. Photochem. Photobiol. B: Biol.*, 1996, **32**, pp.177-181.
9. G. Pfister, R.L. McKenzie, J.B. Liley, A. Thomas, B.W. Forgan and C.N. Long, Cloud coverage based on all-sky imaging and its impact on surface solar irradiance, *J. Appl. Meteorol*., 2003, **42**, pp.1,421-1,434.
10. A.V. Parisi and N. Downs, Cloud cover and eye damaging solar UV exposures, submitted *Int. J. Biomet*., 2004.
11. M.M. Caldwell, Solar ultraviolet radiation and the growth and development of higher plants, in *Photophysiology*, ed. A.C. Giese, **6**, pp.131-177, Academic Press, New York, 1971.
12. S.D. Flint and M.M. Caldwell, A biological spectral weighting function for ozone depletion research with higher plants, *Physiol. Plant.*, 2003, **117**, pp.137-144.
13. R.B. Setlow, The wavelengths of sunlight effective in producing skin cancer: a theoretical analysis, *Proc. Natl. Acad. Sci. USA*, 1974, **71**, pp.3,363-3,366.
14. R.B. Setlow, E. Grist, K. Thompson and A.P. Woodhead, Wavelengths effective in induction of malignant melanoma, *Proc. Natl. Acad. Sci*. 1993, **90**, pp.6,666-6,670.
15. CIE (International Commission on Illumination), Photokeratitis, *CIE J*., 1986, **5**, 19-23.
16. O.M. Oriowo, A.P. Cullen, B.R. Chou and J.G. Sivak, Action spectrum and recovery for in vitro UV-induced cataract using whole lenses, *Invest. Ophthal. Vis. Sci.*, 2001, **42**, 2,596-2,602.
17. F.P. Gasparro, M. Mitchnick and J.F. Nash, A review of sunscreen safety and efficacy, *Photochem. Photobiol.*, 1998, **68**, pp.243-256.
18. A.E.S. Green, T. Sawada and E.P. Shettle, The middle ultraviolet reaching the ground, *Photochem. Photobiol.*, 1974, **19**, pp.251-259.
19. M.M. Caldwell, W.G. Gold, G. Harris and C.W. Ashurst, A modulated lamp system for solar UV-B (280-320nm) supplemental studies in the field, *Photochem. Photobiol.*, 1983, **37**, pp.479-485.
20. A.V. Parisi, J. Sabburg and M.G. Kimlin, Comparison of biologically damaging spectral solar ultraviolet radiation at a southern hemisphere sub-tropical site, *Phys. Med. Biol.*, 2003, **48**, pp.N121-N129.

21. J.D. Longstreth, F.R. de Gruijl, M.L. Kripke, S. Abseck, F. Arnold, H.I. Slaper, G. Velders, Y. Takizawa and J.C. van der Leun, Health risks, *J. Photochem. Photobiol. B: Biol.*, 1998, **46**, pp.20-39.

FIGURE CAPTIONS

Figure 1: An example unprocessed and processed image from the TSI. The white circle on the shadow band is the position of the sun.

Figure 2: (a) Action spectra for DNA damage (1), fish melanoma (2), generalized plant damage (3) and plant damage (4) and (b) the action spectra for cataracts (thin line) and photokeratitis (thick line).

Figure 3: The UVBE for plant damage showing the irradiances for all sky conditions (light shaded symbols) and the irradiances classified as cloud free (dark shaded symbols).

Figure 4: Ratio of measured UVBE to clear sky UVBE for (a) the fish melanoma and (b) the DNA damage action spectra for the cloud enhanced UVBE cases.

Figure 5: Ratio of measured UVBE to clear sky UVBE for the (a) cataracts and (b) photokeratitis action spectra for the cloud enhanced UVBE cases.

Figure 6: Ratio of measured UVBE to clear sky UVBE for the (a) generalized plant damage and (b) plant damage for the cloud enhanced UVBE cases.

Figure 7: Average of the REnh for the different action spectra. The error bars represent the standard error in the mean.

Figure 1: An example unprocessed and processed image from the TSI. The white circle on the shadow band is the position of the sun.

(a)

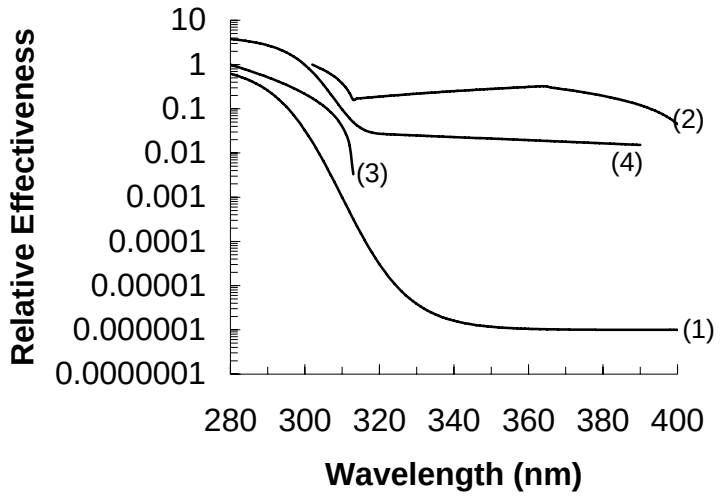

(b)

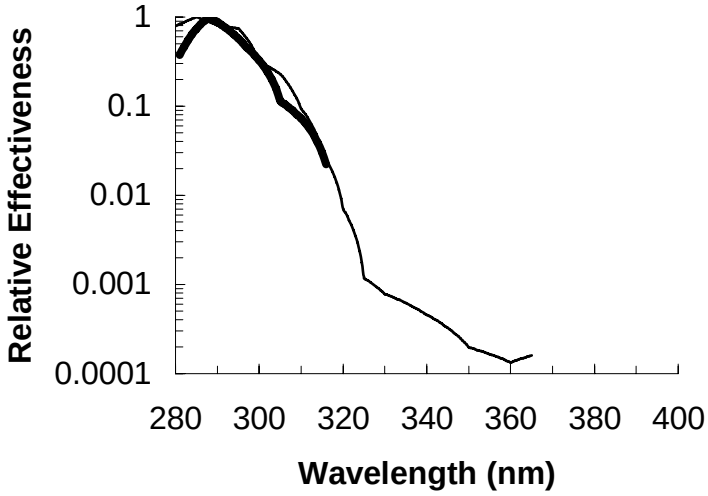

Figure 2: (a) Action spectra for DNA damage (1), fish melanoma (2), generalized plant damage (3) and plant damage (4) and (b) the action spectra for cataracts (thin line) and photokeratitis (thick line).

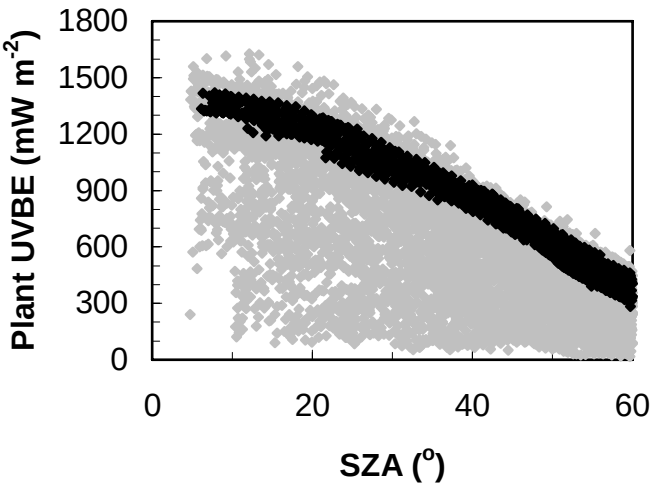

Figure 3: The UVBE for plant damage showing the irradiances for all sky conditions (light shaded symbols) and the irradiances classified as cloud free (dark shaded symbols).

(a)

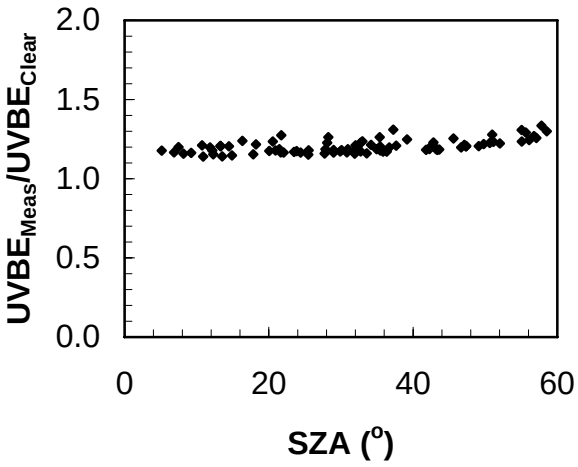

(b)

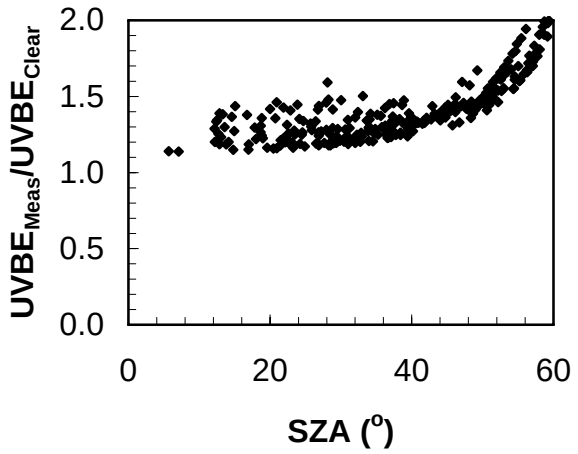

Figure 4: Ratio of measured UVBE to clear sky UVBE for (a) the fish melanoma and (b) the DNA damage action spectra for the cloud enhanced UVBE cases.

(a)

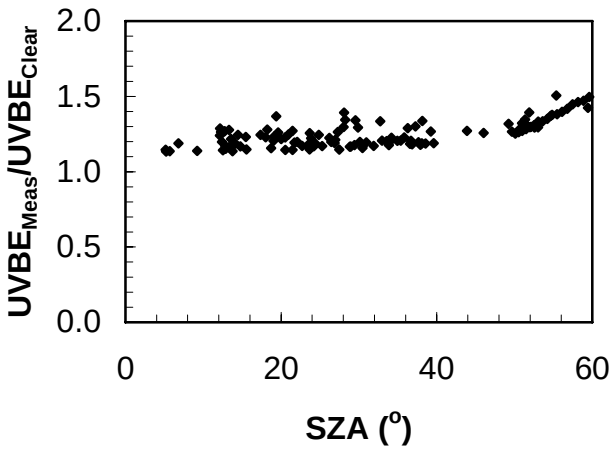

(b)

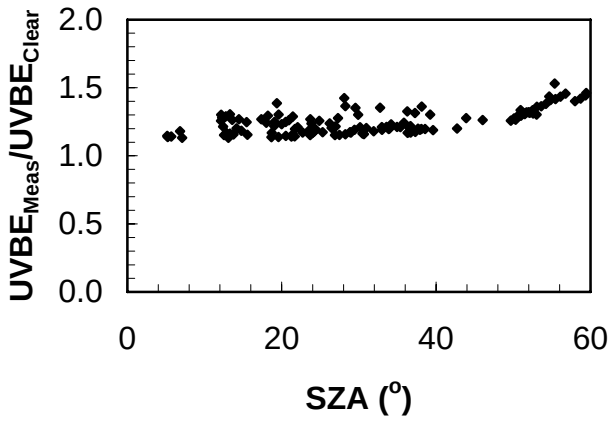

Figure 5: Ratio of measured UVBE to clear sky UVBE for the (a) cataracts and (b) photokeratitis action spectra for the cloud enhanced UVBE cases.

(a)

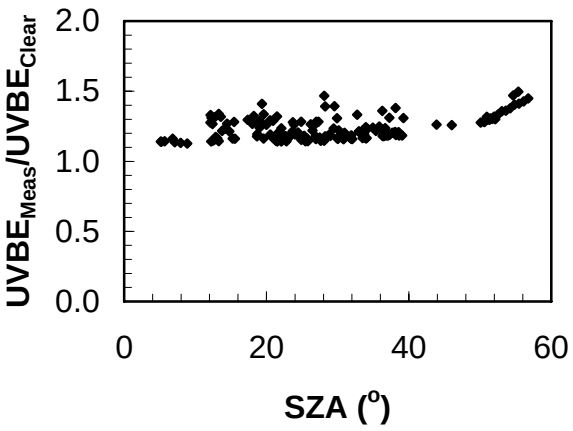

(b)

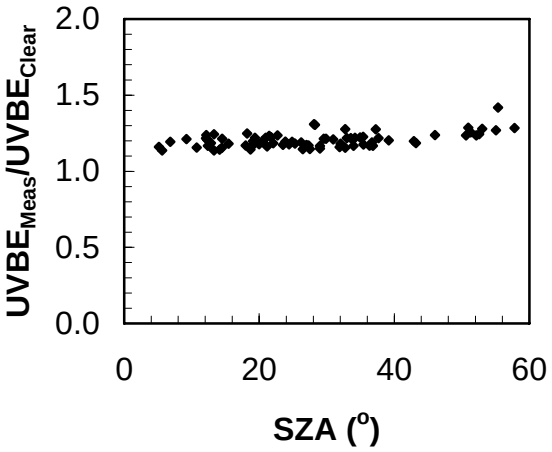

Figure 6: Ratio of measured UVBE to clear sky UVBE for the (a) generalized plant damage and (b) plant damage for the cloud enhanced UVBE cases.

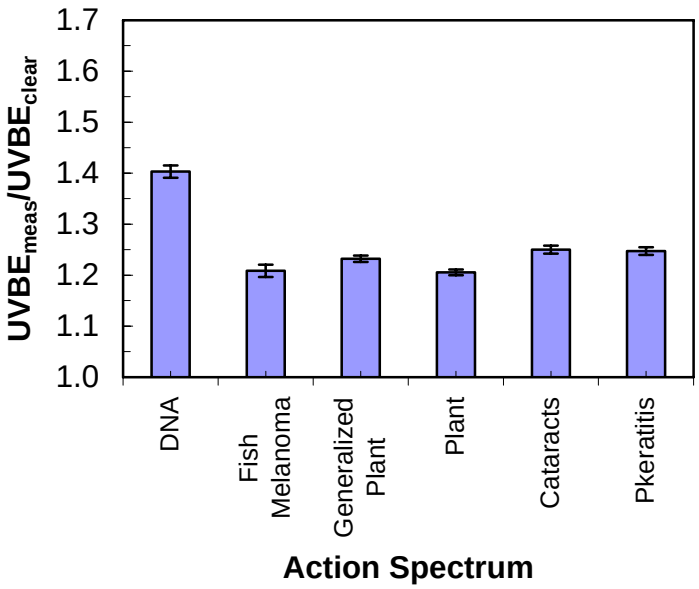

Figure 7: Average of the R_{Enh} for the different action spectra. The error bars represent the standard error in the mean.